Journal of the Brazilian Society of Mechanical Sciences and Engineering (2022) 44:157
https://doi.org/10.1007/s40430-022-03455-5

TECHNICAL PAPER

Adsorption and desorption through packed and fluidized clay-based composite desiccant beds: a comparison study

C. R. Hiremath[1] · Ravikiran Kadoli[2]

Received: 27 January 2021 / Accepted: 19 February 2022

Abstract

The present study considers the composite desiccant employing horse dung, sawdust with clay and later impregnating $CaCl_2$ into the host material. The microscopic and spectroscopic experimental methods such as scanning electron microscope (SEM) and X-ray diffraction (XRD) were used to characterize the composite desiccants. The specific heat (C_p) quantification reveals higher values for clay-additives composite desiccants with lower pore volume and larger grain sizes, whereas lower values for clay composite desiccants with higher pore volume and smaller grain sizes. Adsorption–desorption experiments for moisture removal and addition are conducted in a vertical column in static and fluidized states. The desiccant beds are subjected to an initially set value of process air velocity, relative humidity, temperature and mass of bed. Moisture removal capacity, moisture addition capacity and mass transfer coefficient are the parameter indices adopted to measure the heat and mass transfer characteristics of vertical packed and fluidized bed comprising clay-additives-$CaCl_2$ composite desiccants. Comparing packed and fluidized beds, a higher surface area of bed in fluidization improves dehumidification performance and results in higher desorption rates. Experimental results confirmed that clay and clay-additives-based desiccants have desired adsorption–desorption characteristics of a suitable desiccant. The interesting advantage of fabricated clay and clay-additives-based composite adsorbents is that the air exits the desiccant bed at a lower temperature, saving cooling energy requirements of sorption-based systems.

Keywords Clay · Additives · Composite desiccant · Specific heat · Fluidization

List of symbols

A	Surface area of bed (m^2)
C_p	Specific heat (J/kg K)
d	Diameter (m)
g	Acceleration due to gravity (m/s^2)
K	Convective mass transfer coefficient (m/s)
$\dot{m}$	Mass flux of air (kg/m^2 s)
m	Mass (kg)
P	Pressure (Pa)
R	Gas constant (J/kg K)
S	Humidity ratio of air (g/kg of dry air)
t	Time (s)
T	Temperature (°C)
U	Superficial velocity (m/s)
w	Regression constant

Greek

δ	Small change
μ	Viscosity of air (kg/m s)
ρ	Density (kg/m^3)
τ	Concentration of $CaCl_2$
ϕ	Desiccant pellet

Subscripts

a	Process air
ads	Adsorption
b	Bed
ccl	Calcium chloride
csd	Clay or sawdust or horse dung
des	Desorption
e	Exit
sat	Saturation

Technical Editor: Luben Cabezas-Gómez.

✉ C. R. Hiremath
chandra.hiremath@yahoo.com

Ravikiran Kadoli
rkkadoli@nitk.ac.in

[1] Department of Mechanical Engineering, BLDEA's V. P. Dr. P. G. Halakatti College of Engineering and Technology, Vijayapur, Karnataka 586103, India

[2] Department of Mechanical Engineering, National Institute of Technology Karnataka, Srinivasnagar, Mangalore 575025, India

Published online: 26 March 2022

i	Inlet
s	Bed surface
v	Vapor

Abbreviations

HCFC	Hydrochlorofluorocarbon
HFC	Hydrofluorocarbon
CFC	Chlorofluorocarbon
$CaCl_2$	Calcium chloride
EDAX	Energy dispersive X-ray analysis
MRC	Moisture removal capacity
MAC	Moisture addition capacity
RH	Relative humidity
SEM	Scanning electron microscopy
XRD	X-ray diffraction

1 Introduction

From the environment and energy source perspective, desiccant cooling and dehumidification systems provide an alternative for comfort air conditioning. In traditional air conditioning systems to accomplish dehumidification, atmospheric air is cooled below its dew point and then heated to the desired temperature [1–3]. The dehumidification of supply air in heating, ventilation and air conditioning (HVAC) systems is achieved by refrigerants like HCFC/HFC and refrigerant blends which are alternatives to CFC refrigerants. Although the conventional air conditioning systems do not use ozone-depleting refrigerants, maintaining the balance between thermal comfort, indoor air quality and energy usage is the primary concern. The inefficient and intensive energy utilization affects environmental conservation as most energy is generated from fossil fuels. The desiccant-assisted cooling systems enabled a 1–13% reduction in CO_2 emission and electricity saving of 24% is reported in hot and humid climate conditions of wet markets in Hong Kong. The pre-conditioning of supply air using desiccants can improve the humidity and temperature in air conditioning systems overall energy efficiency and is economically viable [4, 5].

Desiccant air conditioning systems use either hygroscopic salts like chlorides, sulfates, bromides, glycols and nitrates or porous solid sorbents like silica gel, alumina and zeolite. The aforementioned porous solid adsorbents performance depends on porous and thermo-physical properties such as surface area, porosity, pore size, pore volume and specific heat capacity. The nitrogen (N_2) adsorption–desorption data of volumetric adsorption equipment quantify the porous properties of any adsorbent. The specific heat capacity of the desiccant material is one of the prime thermo-physical properties in designing and optimizing sorption cycles. It is measured by direct (adiabatic calorimeters, reaction calorimeters, bomb calorimeters and differential scanning calorimeters (DSC)) and indirect (flash and laser flash) methods. Experimental comparison of thermo-physical and porous properties of six types of commercially available silica gel reveals the highest surface area for regular density (RD) silica gel containing larger particles, whereas lowest pore volume and highest specific heat are quantified for smaller particles. Except for RD-type silica gel, the specific heat is lesser for a particular sample having a larger pore volume [6]. The surface treatment of carbon-based adsorbents induces surface functional groups. The larger particle sizes and surface functional groups contributed to higher heat capacities. The pore structure and surface chemical characteristics affect the water vapor sorption affinity of activated carbon adsorbent [7, 8]. The water vapor adsorption–desorption data on cattle manure compost (CMC)-based activated carbon for water and nitrogen adsorbate depend on pore structure and surface chemical nature. The initial water uptake begins by active acidic sites of functional groups. Weak water–carbon forces cause higher uptake at low relative humidity and water–water forces promote the adsorption of water vapor at high relative humidity. Water adsorption into the pores is predominately by pore volume diffusion and not by capillary condensation mechanism [9]. The performance of the sorption systems can be enhanced by impregnating hygroscopic salts with a porous host matrix. Experimental investigation on the performance of a two-bed adsorption chiller reveals a better cooling capacity for KSK silica gel–calcium chloride (average pore radius of 15 nm) compared to regular density silica gel with water adsorbate [10]. The dynamic sorption analysis of silica gel and silica gel–LiCl composite samples on the water in a thermo-humidistat chamber under the test condition of 20 °C and relative humidity of 70% shows 2–3 times higher sorption capacity for 7–8 nm pore size mesoporous silica gel–LiCl composite desiccant compared to micropore (pore size 2–3 nm) silica gel [1].

Although microphysical and thermo-physical properties of desiccants influence the sorption characteristics the selection of correct desiccant materials, desiccant bed geometry, regeneration are the parameters governing the satisfactory functioning of desiccant-based systems that are likely to solve the problems faced by industries. Fluidized bed desiccation is the most available technology to achieve higher sorption rates. Owing to higher adsorption–desorption rates, lower pressure drop and lower rise in temperature of bed exit air, the effectiveness of the air conditioning system is improved by replacing the silica gel packed bed system. Compared to the packed bed, the total amount of adsorption and desorption increased by 20.8 and 19.8% and also the pressure drop and outlet temperature are reduced by 30 and 36% [11]. The adsorption–desorption performance of laboratory-scale experiments on fixed and fluidized bed silica gel dehumidification unit coupled with rice drying unit reveals higher moisture removal from the rice by

the fluidized bed compared to packed bed dehumidification unit [12].

The commercially available solid and liquid desiccants review has shown good sorption capacity but significantly increases air temperature. However, silica gel has high adsorptivity up to 27% but requires regeneration temperature above 100 °C. Apart from higher regeneration temperature, the carbon footprint added by obtaining silica gel desiccants is 20 times higher than calcium chloride. The increase in air temperature is not desirable in drying temperature-sensitive farm products and increases the sensible heat load of the desiccant-based air conditioning system. It has been revealed that the rise in temperature of process air sorbed by adsorbents prepared by natural materials is low as compared to commercially available silica gel. The comparison of humidity adsorption test on dry coconut coir and silica gel reveals an average increase in silica gel bed temperature by about 65% [13, 14].

The impregnation and mixing of hygroscopic salts with naturally available clay, sand and sawdust produce a new family of composite adsorbents. The effect of carbonization temperature and specific cooling power on sorption capacity and adsorption rate is analyzed for sawdust-$CaCl_2$ composite desiccant and amylum starch for ammonia (NH_3) sorption in adsorption refrigeration applications. Although more pores were induced in the composite above 800 °C, the sorption capacity decreases and the reduction is attributed to the melting of $CaCl_2$ (782 °C) which leads to the blocking of pores [15]. A study on clay-$CaCl_2$ adsorption–desorption characteristics shows the dependence of mass transfer rate on concentration gradient in the bed. For the same operating conditions, desorption rate is higher as compared to the adsorption rate [16]. Investigation on natural absorption of water vapor on the surface of sand–$CaCl_2$ desiccant bed shows the decrease in mass transfer coefficient in the liquid zone of desiccant bed which is attributed to decrease in void volume and the effective mass transfer area [17]. Experimental investigation on water production from atmospheric air using solar regenerated saw wood–60% $CaCl_2$ composite desiccant demonstrates a maximum collection of 180 ml of water/kg/day [18]. The design of a prototype solar regenerative desiccant dehumidifying device employed for drying cereal grains and crops concludes that the fabricated bentonite–$CaCl_2$ desiccants estimated cost was 0.11 times the cost of commercial silica gel [19]. The reported experimental results based on theoretical study reveal the potential of calcium-based clay to adsorb more moisture than sodium-based bentonite at low moisture contents and are preferable for grain drying applications [20].

Citing the desiccation advantages of fluidized bed and sorption performance of desiccants prepared from natural materials, the research explores the possibility of bringing new eco-friendly composite desiccants that can substitute the commercially available chemical desiccants in sorption-based applications. This study aims to employ transported soil, sawdust, horse dung and $CaCl_2$ to fabricate clay-based composite desiccants. Sorption experiments are conducted to find the transient adsorption–desorption characteristics of the vertical packed and fluidized clay-based composite desiccant bed under operating conditions such as inlet air humidity ratio, temperature and bed mass. The influence of pore properties, chemical composition content and specific heat capacity of clay-based adsorbents on water vapor adsorption–desorption characteristics were investigated. This knowledge can help design and develop sorption-based systems essential for drying temperature-sensitive farm products in hot and humid climates.

2 Desiccant preparation and characterization

The transported soil and horse dung are used by the local pot makers in the fabrication of traditional products, such as earthen pots and rural appliances. Sawdust, a by-product of sawmills, is employed as another additive along with horse dung. The transported soil in the clinker form used for pot making was collected from the pot maker and then crushed and ground to obtain the powdered raw material. The soil is gravimetrically analyzed for chemical composition. The main mineral content of transported soil seems similar to the illite clay mineral composition [21]. The chemical composition of the transported soil by weight percentage is presented in Table 1. SiO_2 and Al_2O_3 make up a significant portion of the composition.

The fine powdered form of transported clay is segregated into three parts. The first part of the clay material is without any additives. The second part has 20% horse dung and the third part with 20% sawdust additive by weight. The three portions are mixed with water, resulting in pasty clay and clay-additives material. To make spherical pellets of uniform size, the exact length of material to be cut is estimated by equating the volume of the cylinder and to the volume of the sphere. To mold a 10 mm diameter of spherical pellet, the length of the cylindrical roll cut is 6.67 mm and the corresponding mass is 1.68 g. About 1 kg each of clay, clay-horse dung and clay-sawdust spherical pellets are prepared by hand molding. A cylindrical gauge of 10 mm diameter is employed to ensure the

Table 1 Chemical composition of transported soil by gravimetric analysis

Mineral	SiO_2	Al_2O_3	Fe_2O_3	MgO	CaO	K_2O	Na_2O	Impurities
Weight (%)	51.2	26.4	12.5	3.8	2.1	0.92	0.45	2.63

correct size of pellets produced. To employ the clay with additive material in fluidization studies, cylindrically shaped pellets of 2 mm diameter and 2 mm length are produced. A syringe is used to extrude the pasty clay-additives material. The extrusion procedure produces cylindrical-shaped clay-additives composites. All the green pellets produced are shadow dried for about 24 h.

All the shadow-dried clay, clay-sawdust and clay-horse dung composite desiccants are heated to a maximum weight reduction temperature of 500 °C for about one hour. Subsequently left to cool in the furnace itself and later stored in polythene bags. The dried samples are mixed with an aqueous $CaCl_2$ solution of 50% at room temperature. A soaking period of 24 h is employed to allow diffusion of $CaCl_2$ ions onto the pores of burnt clay and clay-additives composite desiccants. Finally, the impregnated samples are dried at 100 °C and are stored in airtight containers.

A study on the morphologies of the samples was carried out using SEM and EDAX images. A general view of the clay and clay composite can be observed in Fig. 1a, d and g. The micrographs reveal the flaky surface with micro cracks. The textures are highly uneven with the aggregation of grains with interlayer spaces. The surface of the clay was covered with deep pits having higher pore volume (Fig. 1a) while the surface of the clay-horse dung and clay-sawdust being uneven and smooth acquired lower pore volume (Fig. 1d, g). The average surface mesopore diameters are in the order of 6.45, 8.52 and 6.11 μm for

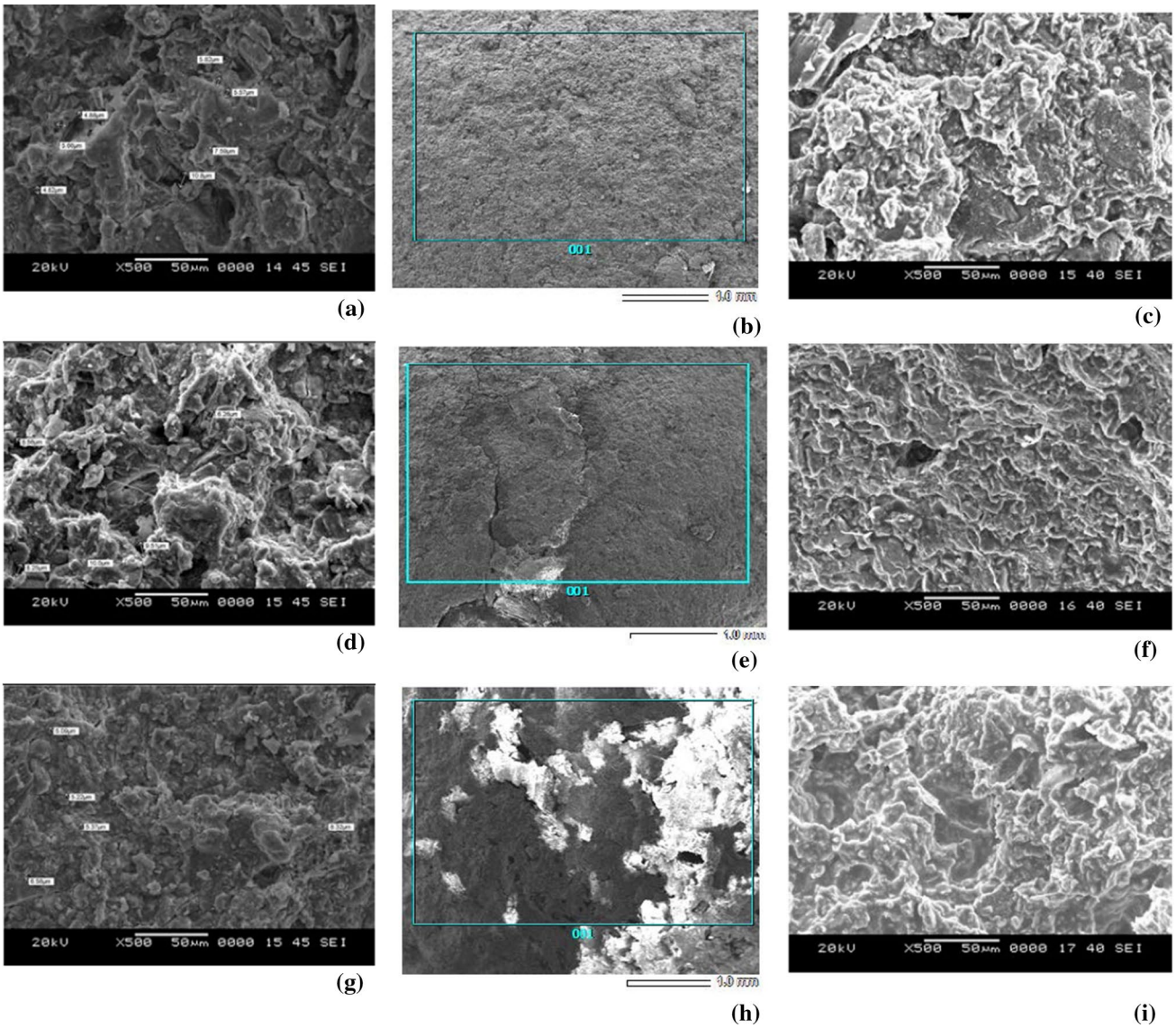

Fig. 1 SEM micrographs, EDAX images and SEM micrographs of $CaCl_2$ impregnated composite desiccants of burnt clay (**a**–**c**), horse dung (**d**–**f**) and sawdust (**g**–**i**)

clay, clay-horse dung and clay-sawdust composite desiccants, respectively. The larger surface pore sizes in clay-additives composites enable a higher surface area than smaller surface pore sizes in clay composites. Figure 1b, e and h presents the two-dimensional micrographs of samples using energy dispersive X-ray analysis. It appears that additives are concentrated in some areas. The dense white patches indicate the dispersion of sawdust in clay in the burnt form (Fig. 1h). The distribution of sawdust is more significant than the distribution of horse dung in clay (Fig. 1e after heat treatment). Figure 1b, d and i shows the micrographs of burnt clay, burnt clay-horse dung and burnt clay-sawdust-$CaCl_2$ composite desiccants. It is observed that nearly the same morphologies are seen with and without impregnation of $CaCl_2$, except that the interlayer spaces are decreased. This may be attributed to the impregnation of $CaCl_2$ between the clay layers.

3 Experimental setup arrangement

Figure 2 shows the schematic arrangement for dehumidification and humidification experiments on the packed and fluidized bed of clay-additives-$CaCl_2$ composite desiccants. The setup consists of an air compressor with reservoir (1), air heating unit (2), orifice meter (3), pressure gauge (4), vertical test section, (5), RH transmitter placed at the bed inlet port and bed outlet port (H1, H2), U-tube differential manometers (M1, M2) and microcontroller interfaced with a computer (6, 7). Air stored in the air reservoir is let flow through the discharge pipeline (Vb1–Vb2) made of polyvinyl chloride. The air flows through the insulated galvanized iron (G I) pressure line (Vg3 to Vb5) from the discharge line and then into the vertical column. The vertical tube is made with a transparent acrylic tube with a height of 700 mm and a diameter of 50 mm. The test section is positioned vertically using a stand. The bottom of the acrylic tube is closed by a sieve plate so that the desiccants can be contained in the tube. The transparent acrylic tube also

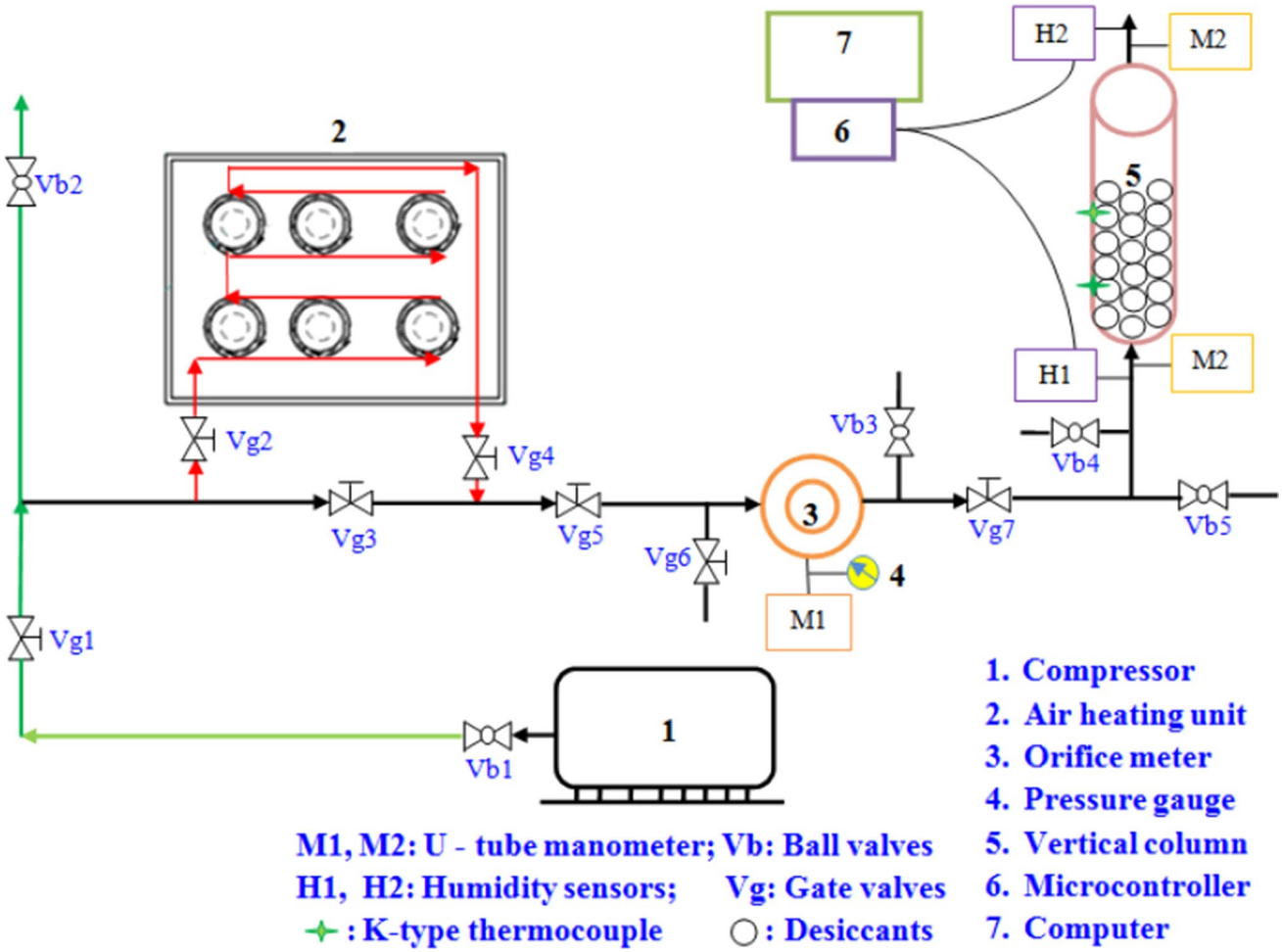

Fig. 2 Schematic layout of the experimental test rig for adsorption–desorption experiments

facilitates the observation of the desiccant pellets in a fluidized state. The vertical column is provided with pressure taps and taps for locating the hygrotransmitter.

The main parameters measured are relative humidity, temperature, pressure drop and mass flow rate of process air during adsorption and desorption experiments. The relative humidity and temperature at bed inlet and exit are measured using calibrated Rotronic make Hygroflex RH transmitter. The transmitter range for measuring relative humidity is from 0 to 100% and temperature is from − 40 to 85 °C. The humidity transmitters at the bed inlet (H1) and exit (H2) are connected to the computer through a microcontroller interface (6). The transient values of relative humidity and temperature of process air are written to excel file for every second of the experiment duration. Water filled U-tube manometer (M1) is connected across orifice meter (3). The diameter of the orifice is 10.12 mm, and the discharge coefficient is 0.68. Flowmeter measures the volume flow rate during the tests. Water filled U-tube manometer (M2) is employed to measure the pressure drop across the packed and fluidized beds.

3.1 Experimental procedure

The packed bed will contain spherical desiccant whose diameter is 10 mm diameter and fluidized bed will contain desiccant in the form of cylindrical pellets having diameter and length 2 mm, respectively. The adsorption and desorption processes for the same combination of bed mass and inlet air velocity for clay-additives-$CaCl_2$ composite desiccants in static and fluidized bed configurations are conducted separately. The ball and gate valves are used to control the airflow. The valve positions for different sets of experiments are shown in Table 2. Air preheating unit (2) is fabricated and arranged to carry out desorption experiments. Six incandescent bulbs of 100 W each are fitted in the air preheater to supply the heat to process air. The performance of the heating unit is checked for different volume flow rates of the process air and regeneration air at constant temperature is passaged into the bed. The maximum steady state air temperature recorded for the regeneration of desiccant beds at bed inlet is 61 °C.

The minimum superficial velocity required for fluidization is calculated using the Leva equation presented below as [22]:

$$U = \frac{7.169 \times 10^{-4} d_{\phi}^{1.82} \left(\rho_{\phi} - \rho_{a}\right)^{0.94} g}{\rho_{\mathrm{a}}^{0.006} \mu_{\mathrm{a}}} \tag{1}$$

The minimum value of fluidization velocity estimated using Eq. (1) ranges from 1.2 to 1.5 m/s. The experimentally tested minimum fluidization velocity for bed weights of 200 and 300 g is from about 1.2–1.7 m/s. Figure 3 shows the detailed views of desiccants in the fluidized state. During the initial period of fluidization, the fluidized bed can be divided into two zones. The upper portion moves upward in a fluidized manner, while the lower bed mass moves in a quasi-static way. As viewed in Fig. 3, when the process air is introduced, the desiccants are slowly moving up and the bed length changes from L1 to L4 in variations of L2, L3 and so on. It is seen that the bubbling of the desiccants is more dominant in the upper region than the desiccants in the lower part of the bed. With time the clay composite desiccants within the bed are set into continuous motion.

4 Performance parameters

The heat and mass transfer characteristics of the given desiccant bed are governed by the parameters like inlet air velocity, relative humidity, temperature and mass of the bed. The performance of the bed is evaluated using the following parameters:

$$C_{p_{\mathrm{b}}} = \left(\frac{m_{\mathrm{ccl}}}{m_{\mathrm{b}}} \times C_{p_{\mathrm{CCl}}}\right) + \left(\frac{m_{\mathrm{csd}}}{m_{\mathrm{b}}} \times C_{p_{\mathrm{csd}}}\right) \tag{2}$$

$$\mathrm{MRC}_{\mathrm{ads}} = \frac{S_{\mathrm{i}} - S_{\mathrm{e}}}{S_{\mathrm{i}}} \tag{3}$$

$$\mathrm{MAC}_{\mathrm{des}} = \frac{S_{\mathrm{e}} - S_{\mathrm{i}}}{S_{\mathrm{e}}} \tag{4}$$

The bed specific heat ($C_{p_{\mathrm{b}}}$), which influences the heat and mass transfer characteristics of desiccant bed, is determined for composite desiccant beds. The difference in mass of desiccants before impregnation (m_{csd}) and after impregnation (m_{b}) gives the mass of $CaCl_2$ (m_{ccl}) impregnated. By knowing the specific heat of $CaCl_2$ ($C_{p_{\mathrm{CCl}}}$) and clay composite desiccants ($C_{p_{\mathrm{csd}}}$) gravimetrically, the bed specific heat values are estimated [23]. The specific heat for burnt clay-$CaCl_2$, burnt clay-horse dung-$CaCl_2$ and burnt clay-sawdust-$CaCl_2$ composite desiccant beds are 2307.97, 4468.88 and 5036.41 J/kg K, respectively. The dehumidification ($\mathrm{MRC}_{\mathrm{ads}}$) and

Table 2 Status of valves for humidification and dehumidification processes

Valves process	Vb1	Vb2	Vb3	Vb4	Vb5	Vg1	Vg2	Vg3	Vg4	Vg5	Vg6	Vg7
Adsorption (pressure line)	1	0	0	0	0	1	0	1	0	1	0	1
Desorption (air heating unit)	1	0	0	0	0	1	1	0	1	1	0	1

0 Valves closed, *1* valves opened, *b* ball valve, *g* gate valve

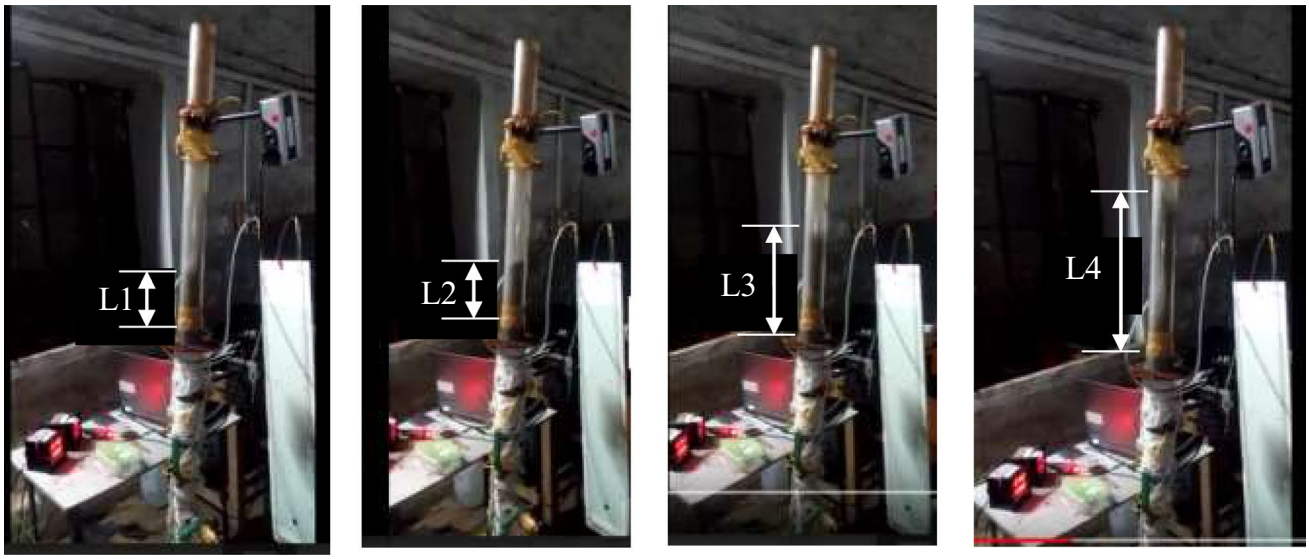

Fig. 3 Photographs of clay-$CaCl_2$ composite desiccant particles in fluidized condition

humidification ability (MAC_{des}) are estimated using inlet and exit air humidity ratio. The analysis of the mass transfer coefficient is investigated using the bed mass, the density of water vapor in the air and at bed surface. The convective mass transfer coefficient (K) is estimated using Eqs. (5)–(8):

$$K = \frac{(\dot{m}_{\mathrm{v}})}{\left(\rho_{v_{\mathrm{i}}} - \rho_{v_{\mathrm{i}}}\right)} \tag{5}$$

$$\dot{m}_{\mathrm{v}} = \frac{\delta m_{\mathrm{b}}}{A\delta t} \tag{6}$$

$$\rho_{v_{\mathrm{i}}} = \frac{P_{v_{\mathrm{i}}}}{RT_{a_{\mathrm{i}}}} \tag{7}$$

$$\rho_{v_{\mathrm{s}}} = \frac{P_{v_{\mathrm{s}}}}{RT_{\mathrm{s}}} \tag{8}$$

The vapor pressure at desiccant bed inlet ($P_{v_{\mathrm{i}}}$) is a function of relative humidity (RH_{i}) and saturation pressure (P_{sat}) which is a function of temperature of air and is given by Tetens equation as

$$P_{\mathrm{sat}} = 610.78 \times \mathrm{e}^{\frac{(17.2694 \times T_{a_{\mathrm{i}}})}{(T_{a_{\mathrm{i}}} + 273)}} \tag{9}$$

The vapor pressure ($P_{v_{\mathrm{i}}}$) of air at bed inlet is estimated using the equation

$$P_{v_{\mathrm{i}}} = \mathrm{RH}_{\mathrm{i}} \times P_{\mathrm{sat}} \tag{10}$$

The value of vapor pressure at bed surface ($P_{v_{\mathrm{s}}}$) is estimated using the data extracted from the $CaCl_2$-water vapor chart [24]. A four-degree polynomial relating to the vapor pressure ($P_{v_{\mathrm{s}}}$) in mmHg and $CaCl_2$ concentration (τ) is obtained. For the $CaCl_2$ concentration of $\tau = 0$ to 50% and for the temperatures of 20 and 40 °C, the regression constants (w_0 to w_4) are furnished in Table 3. The vapor pressure ($P_{v_{\mathrm{s}}}$) in Pascal is given by

$$P_{v_{\mathrm{s}}} = (w_0 + w_1\tau + w_2\tau^2 + w_3\tau^3 + w_4\tau^4) \times (13.6 \times 9.81) \tag{11}$$

5 Uncertainty analysis

Before analyzing the experimental results, the experimental uncertainties of parameters are estimated and the sample uncertainties of different evaluated parameters are presented in Table 4 [25–27]. It can be noted that though the same devices are used for the measurement of air relative

Table 3 Regression constants for relating vapor pressure and temperature of $CaCl_2$

Temperature	20 °C	40 °C
Regression constants		
w_0	17.86085149	53.0389912
w_1	− 0.1534159594	0.03443817921
w_2	0.0006167150232	− 0.0352294261
w_3	− 0.0001772467701	0.0003926850743
w_4	$2.283595335 \times 10^{-6}$	$-4.475770425 \times 10^{-7}$

humidity and temperature at bed inlet and exit, the uncertainty involved differs. This is because for the given conditions, device uncertainty is fixed, but the uncertainty involved in the measured value is a function of other parameters, which increases the propagation of uncertainty. The higher value of uncertainty for humidity ratio in adsorption and desorption experimental runs is ± 8%.

6 Analysis of experimental results

Basic experiments are conducted to analyze the heat and mass transfer characteristics of clay and clay-additives-based composite desiccant. The experimental results for packed and fluidized beds are compared concerning air humidity ratio, temperature, bed mass and mass transfer coefficient in adsorption and desorption modes. The sorption properties of clay and clay-additives composite adsorbents are influenced by operational parameters, pore properties, surface chemical content and thermo-physical properties such as bed-specific heat. Figure 4a, c, e presents the quantitative EDAX elemental composition of burnt clay, burnt clay horse dung and burnt clay-sawdust samples. The results of EDAX analysis agree with the results of the mineral study of raw clay shown in Table 1. The quantitative analysis of the EDAX spectrum shows a high content of silicon (Si) and the presence of other alkali and alkaline elements like carbon (C), sodium (Na), magnesium (Mg), aluminum (Al), calcium (Ca) and iron (Fe).

As shown in Fig. 4b, d, f, a similar X-ray diffraction pattern is observed for all the three clay-$CaCl_2$ composite desiccants. The high intensity of diffraction peaks indicates good crystalline nature. The crystalline XRD pattern indicates the porous nature of clay-additives composite desiccant. The reflections corresponding to planes show the planes of the presence of elemental oxides. The other smaller peaks correspond to other minerals present in clay-additives and clay-additives-$CaCl_2$ samples. Debye–Scherrer's equation [28] is used to calculate the average crystallite size of the clay and clay-additives-based composite desiccants. The average crystallite size for clay-additives particles is 53.49–1.46 nm. For synthesized **c**lay-based composite, desiccants are from 42.75 to 9.25 nm. The higher specific heat capacity [from Eq. (2)] of clay-additives desiccants than clay desiccants is attributed to larger crystal sizes, lower pore volume and higher surface area.

6.1 Adsorption characteristics of vertical packed and fluidized bed of burnt clay-additives-$CaCl_2$ composite desiccants

The test results of the packed bed and fluidized bed systems in adsorption are presented in Table 5. The experimental time variation of exit air humidity ratio and temperature with respect to inlet air velocity to the bed, humidity ratio, temperature and mass of bed through a packed and fluidized bed of burnt clay-$CaCl_2$ and burnt clay-additives-$CaCl_2$ desiccants are shown in Figs. 5, 6, 7, 8 and 9.

The packed bed and fluidized bed system test results in adsorption demonstrate similar trends for transient variation of exit air humidity ratio and temperature are observed as that of runs corresponding to clay-$CaCl_2$, clay-horse dung-$CaCl_2$ and clay-sawdust-$CaCl_2$ composite desiccant beds. For all the three desiccant beds, as shown in Figs. 5a, 6a, 7a, 8a and 9a, the maximum reduction in moisture content of air occurs within a short period of adsorption. The air loses its moisture to the bed and leaves at a minimal humidity ratio. After a short period (about 500 s) of the process, the decrease in surface energy results in the release of adsorption heat that increases the bed surface temperature (24–29 °C) with respect to process air inside the bed. According to the Le Chatelier principle, the change in bed temperature lowers the adsorption capacity and is indicated by the rise in exit air temperature and humidity ratio. Progressing in time, water vapor diffusion in mesopores further increases the bed water content. With the accumulation of water, the increase in the equivalent specific heat of the bed and water gradually decreases the temperature of bed exit air and steadily reaches the minimum value. The experimental tests reveal that though there is an increase in exit air temperature, the rise is below the bed inlet air temperature.

Table 4 Uncertainty values in the evaluated parameters

Parameter	Uncertainty (%)			
	At bed inlet		At bed exit	
	Run1 (adsorption)	Run8 (desorption)	Run1 (adsorption)	Run8 (desorption)
Saturation pressure (P_{sat})	± 0.8336	± 0.6421	± 7.7180	± 2.6534
Vapor pressure (P_v)	± 1.3019	± 0.7749	± 7.8021	± 2.8685
Humidity ratio (S)	± 1.3135	± 0.7769	± 7.8455	± 2.8846
Superficial velocity (U)	± 0.24% @ U = 1.74 m/s			
Mass of bed (m_b)	± 0.0033% @ m_b = 300 g			
Specific heat of bed (C_{p_b})	± 1.0033%			

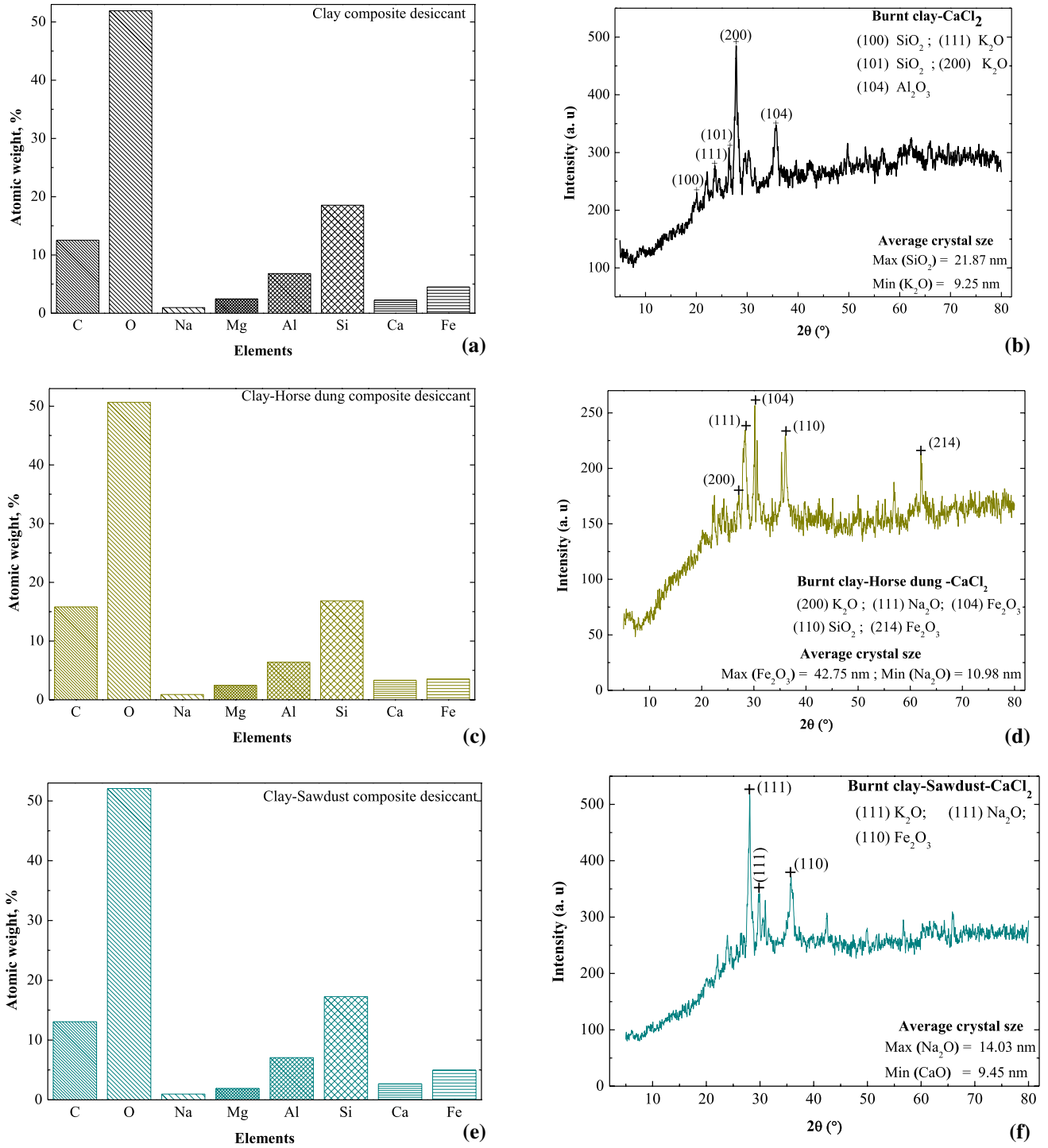

Fig. 4 EDAX images and XRD spectrum depicting elemental analysis of burnt clay (**a**, **b**), horse dung (**c**, **d**) and sawdust (**e**, **f**) composite desiccants

The mineral composition and EDAX spectrum indicate high composition silicon (Si). The hydrothermal stability of the silicon layer impedes the formation of silanol, which has high hydrogen bond formation energy [14]. Apart from hydrothermal stability of silica dioxide, higher heat capacity (2000 to 5000 J/kgK) of clay and clay-additives composite desiccants beds, the heat energy evolved is dissipated in the composite desiccants bed that results in a lesser rise in temperature of exit air with respect to bed inlet air moisture content and temperature. In the case of a fluidized bed, the increase in the amount

Table 5 Experimental observations for packed and fluidized beds in the adsorption process

Run	Composite desiccant bed	Process	Mass of bed (g)	Velocity (m/s)	Pressure drop (Pa)	Increase in bed water content (%)	Process time (seconds)	Atmospheric air	
								Humidity ratio (g/kg)	Temperature (°C)
1	Clay (packed)	Ads	300	2	372.78	2.18	7379	9.83	24.5
1a	Clay (fluidized)	Ads	300	2	519.93	3.40			
2	Horse dung (packed)	Ads	200	1.5	241	2.6	2852	9.55	25
2a	Horse dung (fluidized)	Ads	200	1.5	943	4.00			
3	Horse dung (packed)	Ads	300	2	470.88	2.4	6102	10.92	21.3
3a	Horse dung (fluidized)	Ads	300	2	490.5	2.93			
4	Sawdust (packed)	Ads	200	1.5	323	2.42	4359	10.76	21
4a	Sawdust (fluidized)	Ads	200	1.5	372.78	4.46			
5	Sawdust (packed)	Ads	300	2	451.26	1.98	2926	9.74	24.8
5a	Sawdust (fluidized)	Ads	300	2	1226.25	2.22			

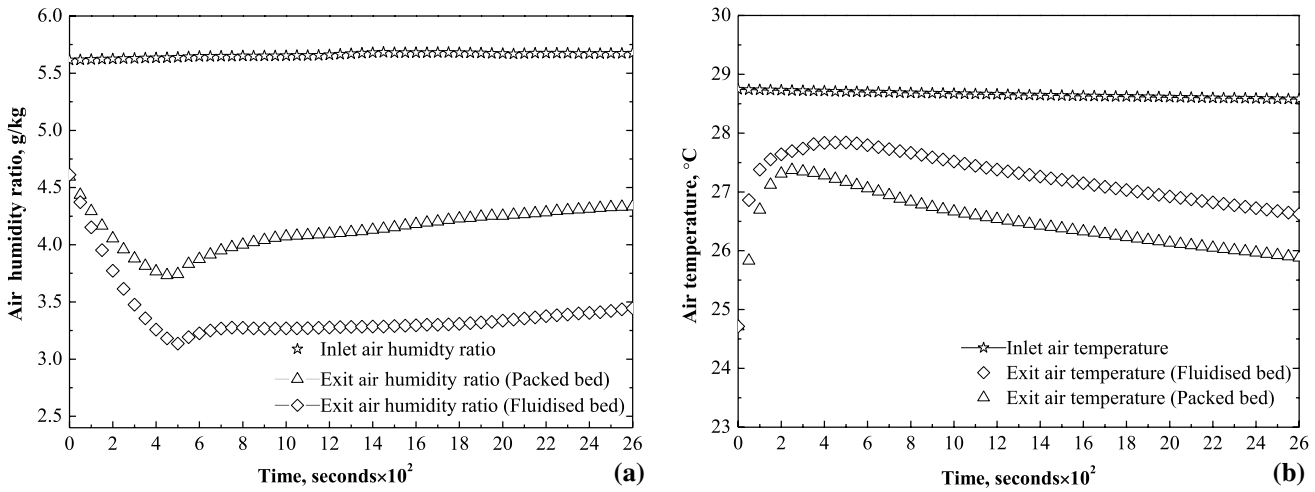

Fig. 5 Transient variation of process air **a** humidity ratio and **b** temperature showing to run1 and run1a, clay-$CaCl_2$ composite desiccant bed in adsorption

of air passing through the bed per unit time and higher surface area of the bed enhances the adsorption rate. Figures 5b, 6b, 7b, 8b and 9b reveal a lower degree of temperature rise in fluidized bed as compared to packed bed. The higher adsorption rates and heat dissipation in fluidized beds increase the exit air temperature compared to the packed bed.

6.2 Desorption characteristics of vertical packed and fluidized bed of burnt clay-additives-$CaCl_2$ composite desiccants

Table 6 lists the parameters for different runs of experiments in desorption. The temperature of the air used for regeneration ranges from 48 to 55 °C. Figures 10, 11, 12, 3, 14 and 15 compare the desorption process of all three types of clay additives based on composite desiccant particles in packed and fluidized process modes.

Comparing the desorption rates of packed and fluidized beds (Fig. 10a), initial intense increase in moisture content with time followed by a gradual decrease in moisture content of process air for packed bed as compared to fluidized bed occurs. In a packed bed, the desorption rate gradually decreases and steadily reaches the minimum value. Due to higher mixing and circulation, the desorption rate in fluidized bed sharply increases and reaches the minimum value within 750 s of process time. Within this period, the exit air

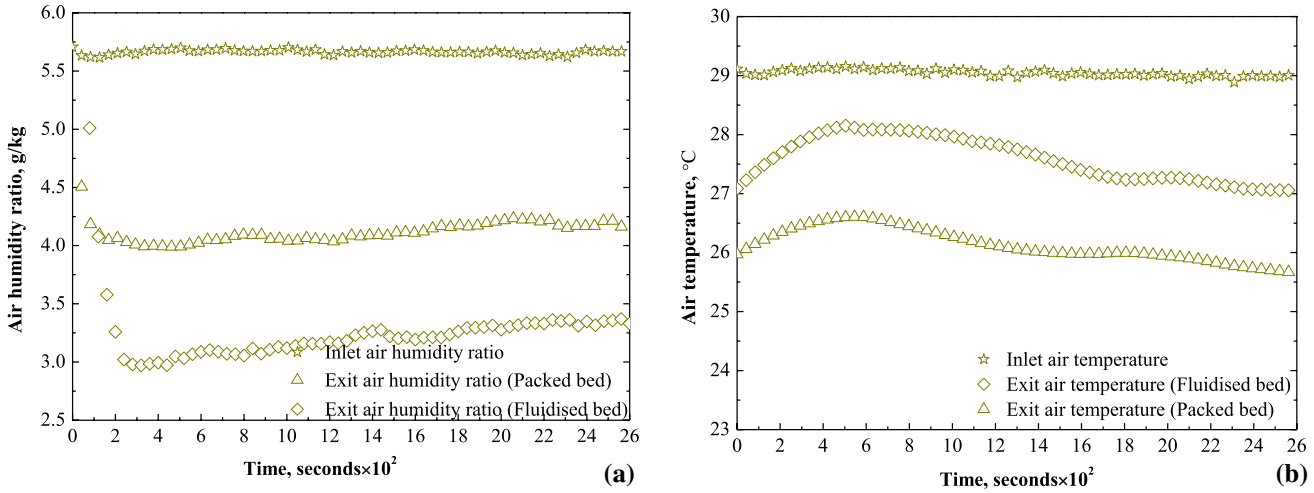

Fig. 6 Transient variation of process air **a** humidity ratio and **b** temperature related to run2 and run2a, clay-horse dung-$CaCl_2$ composite desiccant bed in adsorption

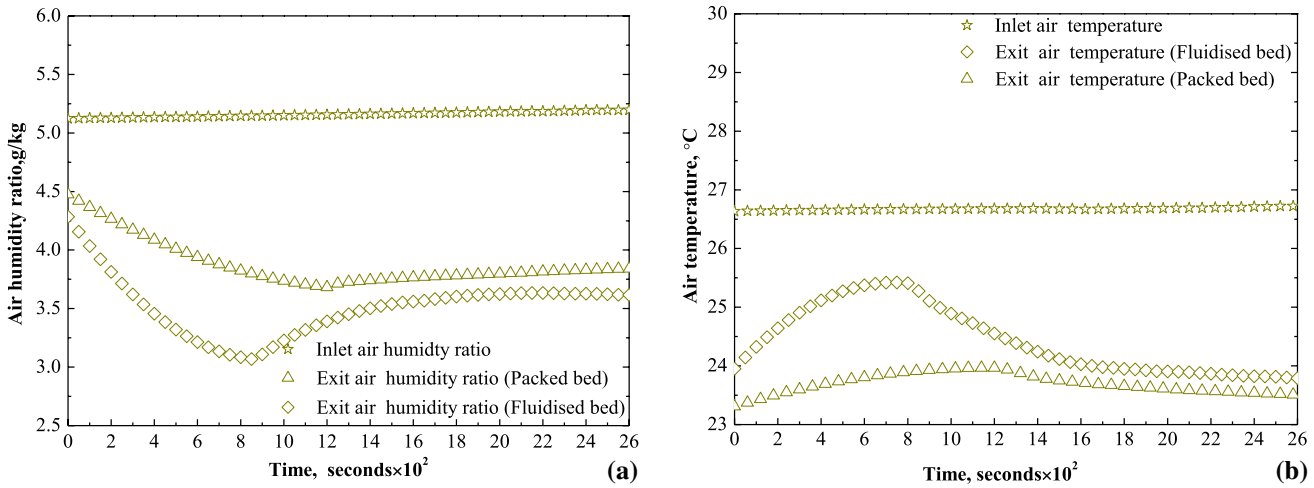

Fig. 7 Transient variation of process air **a** humidity ratio and **b** temperature illustrating run3 and run3a, clay-horse dung-$CaCl_2$ composite desiccant bed in adsorption

humidity ratio for fluidized bed reaches the inlet air humidity ratio and thereby reaches saturation. The exit air temperature increases beyond saturation point (950 s) and then progresses with steady-state temperature (Fig. 10b). In the experimental run (Fig. 11), the desorption rate in packed and fluidized beds gradually decreases. The circulation in the fluidized bed is not adequate, which deteriorates the mass transfer rates on the desiccant surface to air. Due to poor circulation, the hot spots may not be dissipated uniformly throughout the fluidized bed. So desorption rate in the fluidized bed is nearly the same as the packed bed desorption rate. As depicted in Figs. 12a, 13a, 14a and 15a, because of the lower void volume of bed and higher heat capacities, the packed bed desorption rate lags behind the fluidized bed desorption rate. With time the humidity ratio of air exiting the bed reaches the inlet air humidity ratio and drops to its minimum; thereby, equilibrium of moisture content between bed inlet and exit air for both packed and fluidized beds is attained. At dynamic equilibrium, the completely dried beds are further exposed to hot regeneration air. To counterbalance the changes applied to the equilibrium state, the previous process of desorption is shifted to adsorption [Le Chatelier principle]. Due to this, the mass transfer potential will be changed from air to desiccant bed and the bed will take moisture from the air and prevail in adsorption mode. The temperature profiles as presented in Figs. 12b, 13b, 14b and 15b show the increase in temperature of bed exit air and enhancement in temperature of air proceeded up to the time of saturation is due to heat of desorption. Because of lesser voids and higher specific heat capacity, prevailing in

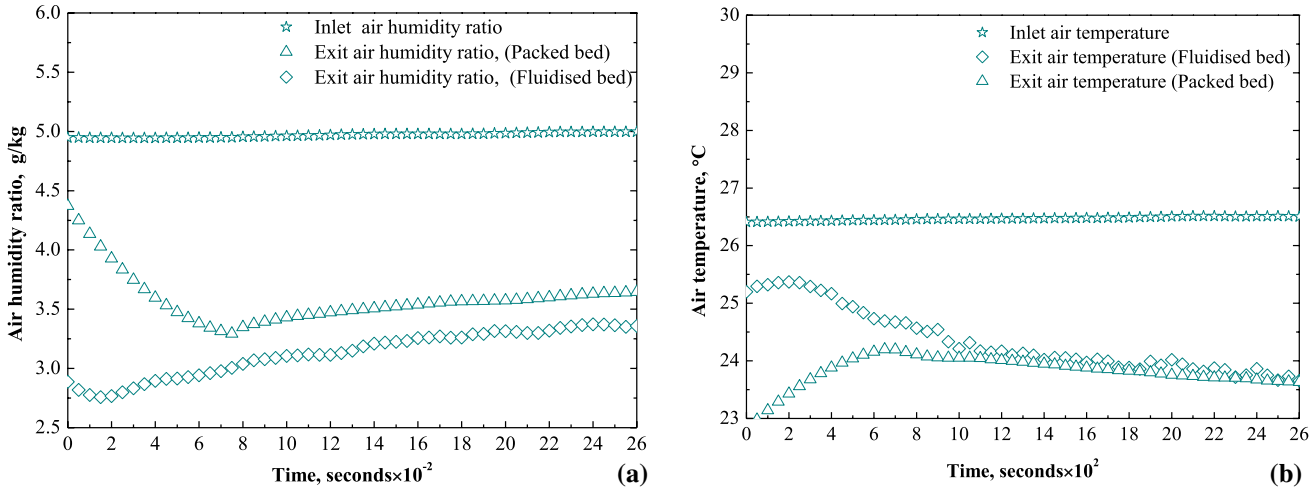

Fig. 8 Transient variation of process air **a** humidity ratio and **b** temperature presenting to run4 and run4a, clay-sawdust-$CaCl_2$ composite desiccant bed in adsorption

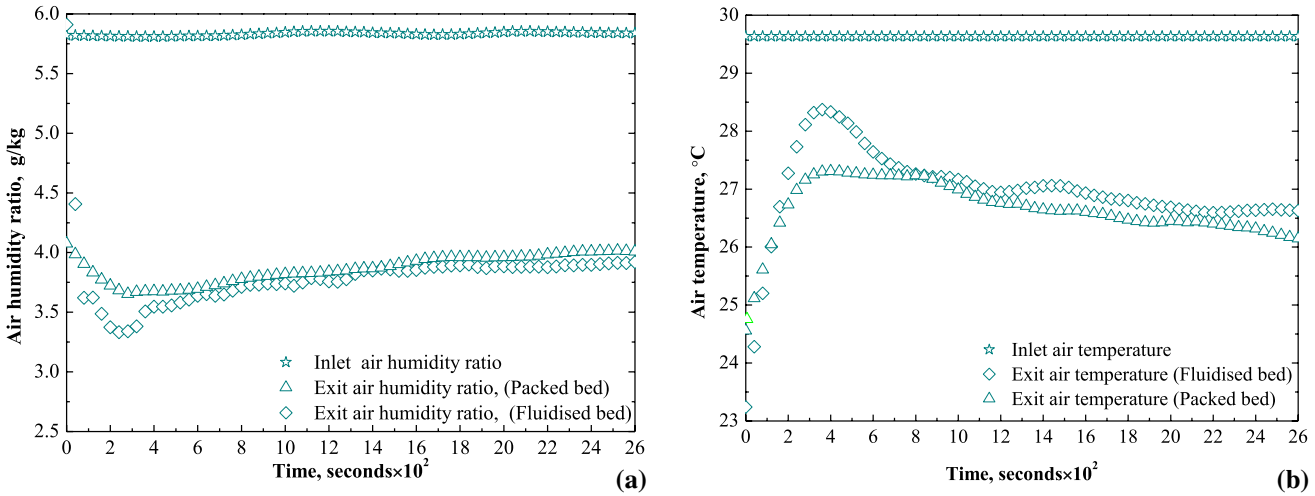

Fig. 9 Transient variation of process air **a** humidity ratio and **b** temperature corresponding to run5 and run5a, clay-sawdust-$CaCl_2$ composite desiccant bed in adsorption

packed bed results in a marginally lower increase in exit air temperature than the fluidized bed.

6.3 Comparison of vertical packed and fluidized bed of burnt clay-additives-$CaCl_2$ composite desiccants for moisture removal and moisture addition capacity

Moisture removal capacity in the adsorption process evaluated using Eq. (3) is presented in Fig. 16a and b for a packed and fluidized bed. The adsorption capability is being compared using three composite desiccants. The inlet velocity of the process air to the bed is 2 m/s and the mass of the bed is 300 g. The whole process is categorized into three zones for all three packed and fluidized beds. The process dynamics for the fixed time can be divided into three zones, namely fast dynamics, medium dynamics and slow dynamics. In the first region, which is from 0 to 550 s, removing moisture from the process air by the packed and fluidized beds is too rapid. The peak value of moisture removal is attained at about 500 s. The initial water content of clay composite desiccants is 6% which is lower than the 11–15% of clay-additives composite desiccants water content. The addition of additives induces micro-cracks of higher pore sizes in clay-additives desiccants. The larger surface pore sizes (SEM micrographs) and crystal sizes (XRD patterns) resulted in moisture uptake by specific adsorption sites in clay-additives composite desiccants. For the identical conditions, the number of adsorption sites exposed to low humidity air seems to be more in clay desiccant bed. The lower

Table 6 Experimental observations for packed and fluidized beds in the desorption process

Run	Composite desiccant bed	Process	Mass of bed (g)	Velocity (m/s)	Pressure drop (Pa)	Decrease in bed water content (%)	Process time (s)	Atmospheric air	
								humidity ratio (g/kg)	Temperature (°C)
6	Clay (packed)	Des	200	1.5	245.25	1.9	2907	9.39	27
6a	Clay (fluidized)	Des	200	1.5	49.05	2.9			
7	Sawdust (packed)	Des	200	1.5	539.55	1.2	3353	9.41	26.7
7a	Sawdust (fluidized)	Des	200	1.5	49.05	2.9			
8	Sawdust (packed)	Des	300	2	598.41	1.5	2471	9.48	28
8a	Sawdust (fluidized)	Des	300	2	122.63	1.8			
9	Horse dung (packed)	Des	200	1.5	245.63	0.5	5406	10.09	24.8
9a	Horse dung (fluidized)	Des	200	1.5	19.62	1.0			
10	Horse dung (packed)	Des	300	1.5	274.68	1.3	5158	12.25	29
10a	Horse dung (fluidized)	Des	300	1.5	39.24	2.0			
11	Horse dung (packed)	Des	300	2	559.17	1.8	3104	9.79	29
11a	Horse dung (fluidized)	Des	300	2	29.43	2.9			

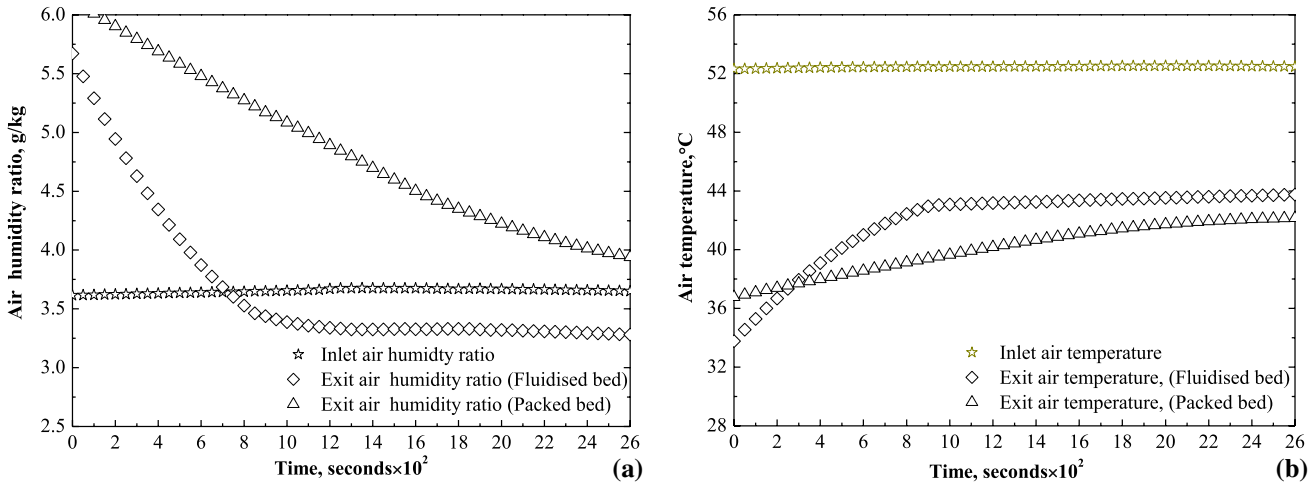

Fig. 10 Transient variation of process air **a** humidity ratio and **b** temperature depicting run6 and run6a, clay-$CaCl_2$ composite desiccant bed in desorption

initial water content, higher pore volume and higher adsorption sites of clay composite desiccant bed may result in more potential for moisture adsorption from the low humidity process air. At the end of the first zone, the release of adsorption heat suddenly decreases the moisture removal capacity. In a medium dynamics region from about 550–2000s, the uptake by the clay composite desiccant beds is steadily progressing. In the medium dynamics region, clear demarcation of the adsorption process can be identified and due to higher pore and grain sizes, the decrease is more pronounced in additives beds. In the third region, due to the accumulation of water in the bed, the moisture removal capacity of

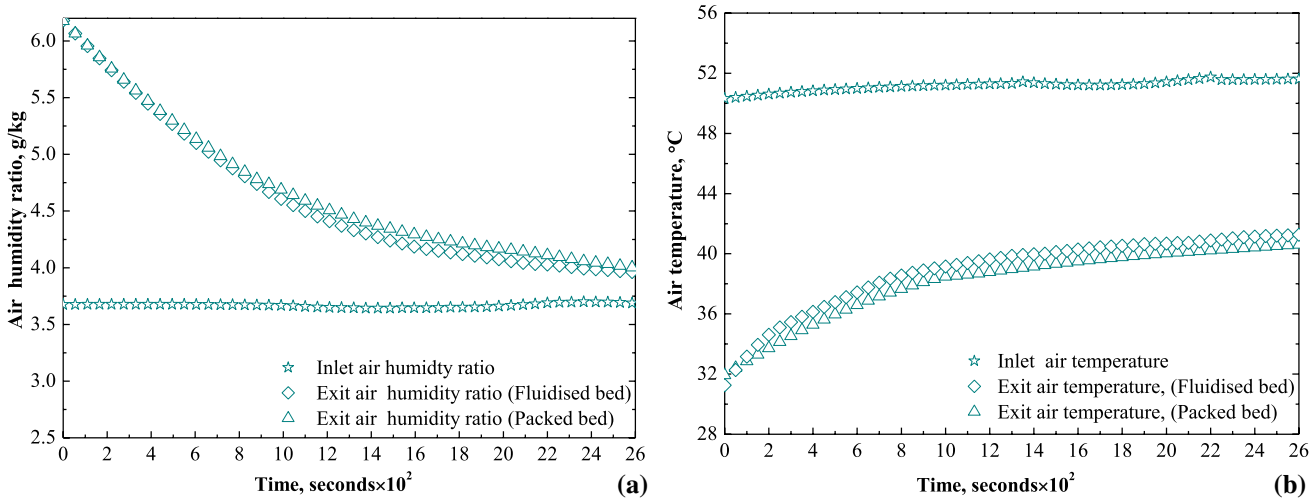

Fig. 11 Transient variation of process air **a** humidity ratio and **b** temperature corresponding to run7 and run7a, clay-sawdust-$CaCl_2$ composite desiccant bed in desorption

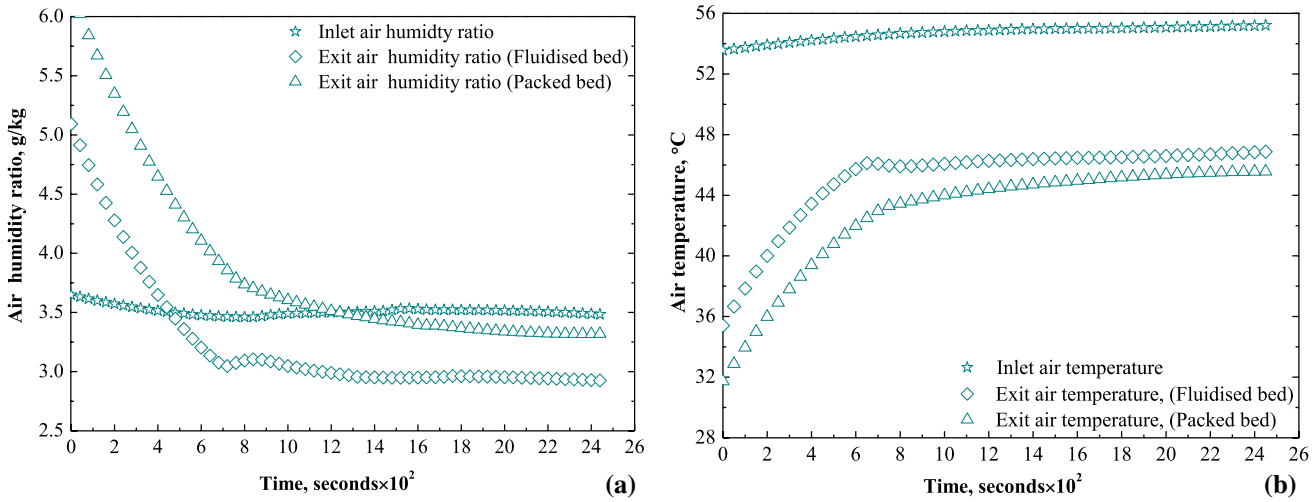

Fig. 12 Transient variation of process air **a** humidity ratio and **b** temperature related to run8 and run8a, clay-sawdust-$CaCl_2$ composite desiccant bed in desorption

beds further decreases compared to adsorptive power in the second region.

Moisture addition capacity in the desorption process is evaluated using Eq. (4). For the bed inlet velocity of 1.5 m/s and mass of bed as 200 g, the whole desorption process can be divided into three zones in packed and fluidized beds, as shown in Fig. 17a and b. The bed inlet air temperature is 52 °C and relative humidity is 5.3%. In the first zone, the clay composite desiccant beds operate in desorption mode, while in the second and third zones, the beds operate in adsorption mode. Owing to the higher vapor pressure on the bed surface (2461.78 Pa) compared to process air vapor pressure (939.65 Pa), the rate of desorption is rapid in the first fast dynamic zone. Comparing the humidification capacity of the beds in the packed bed mode of operation, it seems that burnt clay-$CaCl_2$ and burnt clay-horse dung-$CaCl_2$ composite desiccant beds are completely dried before the end of 750 s and the adsorption sites are contained with hygroscopic $CaCl_2$ void of water. Though additive beds have higher specific heat, higher desorption rates may be attributed to weak adhesive forces between the desiccant surface and the adhered water molecules. After the process time of 750 s, the composite desiccant beds operate in adsorption mode. However, the burnt clay-sawdust-$CaCl_2$ desiccant bed continues to desorb until 3400 s. The saturation time for all desiccant materials is different and further exposure of

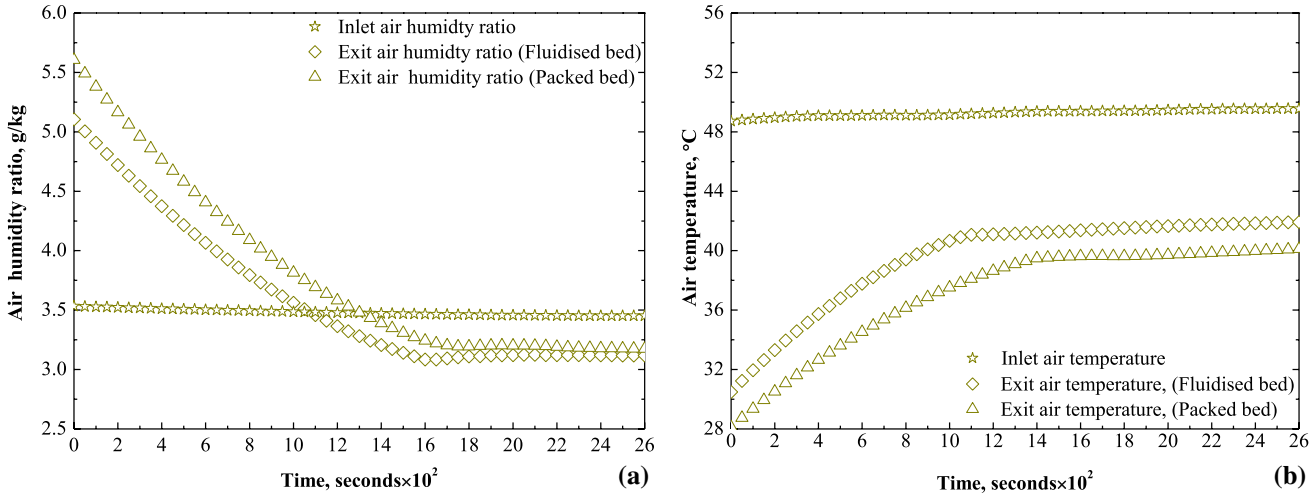

Fig. 13 Transient variation of process air **a** humidity ratio and **b** temperature corresponding to run9 and run9a, clay-horse dung-$CaCl_2$ composite desiccant bed in desorption

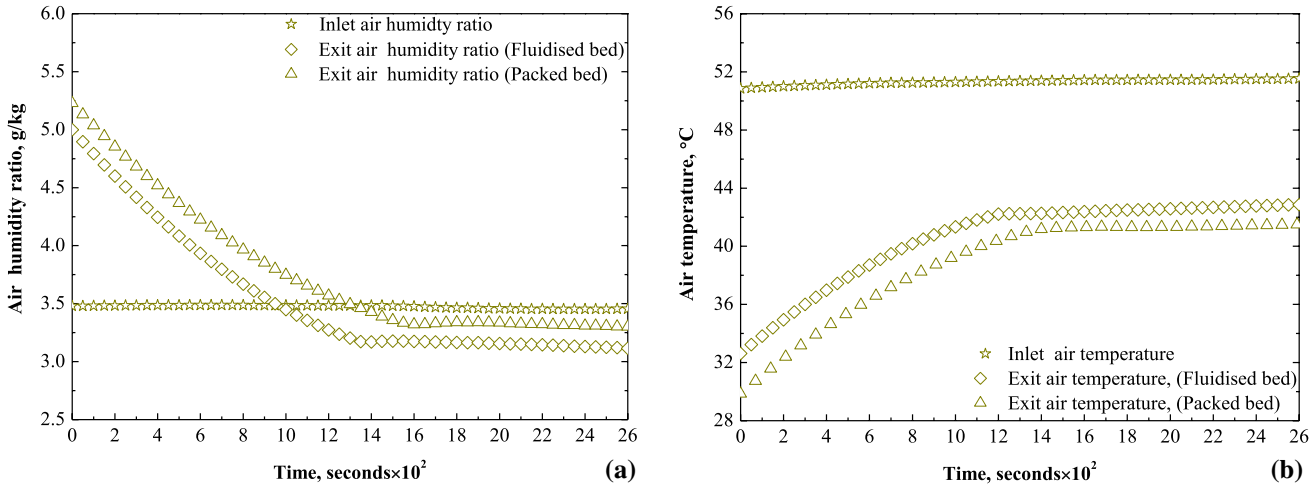

Fig. 14 Transient variation of process air **a** humidity ratio and **b** temperature corresponding to run10 and run10a, Clay-Horse dung-$CaCl_2$ composite desiccant bed in desorption

equilibrium state to change in bed temperature and specific heat capacity reverses the process dynamics from desorption to adsorption mode.

6.4 Analysis of mass transfer coefficient

The mass transfer potential in terms of mass transfer coefficient for the convective mass transfer process is calculated by using Eqs. (5)–(8). The mass transfer coefficient in terms of transverse velocity for different runs in adsorption and desorption is presented in Figs. 18, 19 and 20.

The change in mass transfer coefficient during adsorption and desorption processes can be attributed to change in thermophysical properties and bed operating characteristics of process air in packed and fluidized beds. In the early stages of the process, the mass transfer coefficient has higher values at the beginning of adsorption (Figs. 18a, 19a, 20a) and decreases nearly to a constant value. Initially, due to higher specific surface area, lower air side resistance, the lower specific heat of the bed will enhance mass transfer potential and increase the mass transfer coefficient. With time the accumulation of water vapor in the bed decreases the effective volume of the bed for adsorption and increases the resistance to moisture diffusion into the pores. The decreased interstitial volume of bed, higher specific heat and higher resistance to diffusion of water vapor into the pores reduce the mass transfer coefficient and steadily reach its minimum value. Compared to packed beds, higher mass transfer coefficient values prevail in fluidized beds. During the initial period of fluidization, the visualization of the fluidized bed shows the

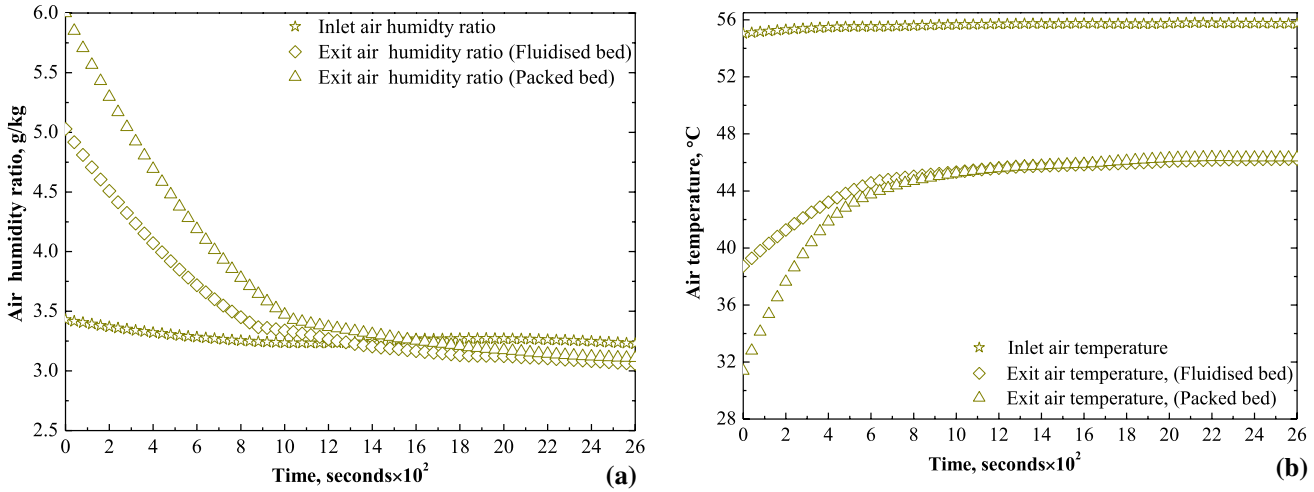

Fig. 15 Transient variation of process air **a** humidity ratio and **b** temperature corresponding to run11 and run11a, clay-horse dung-$CaCl_2$ composite desiccant bed in desorption

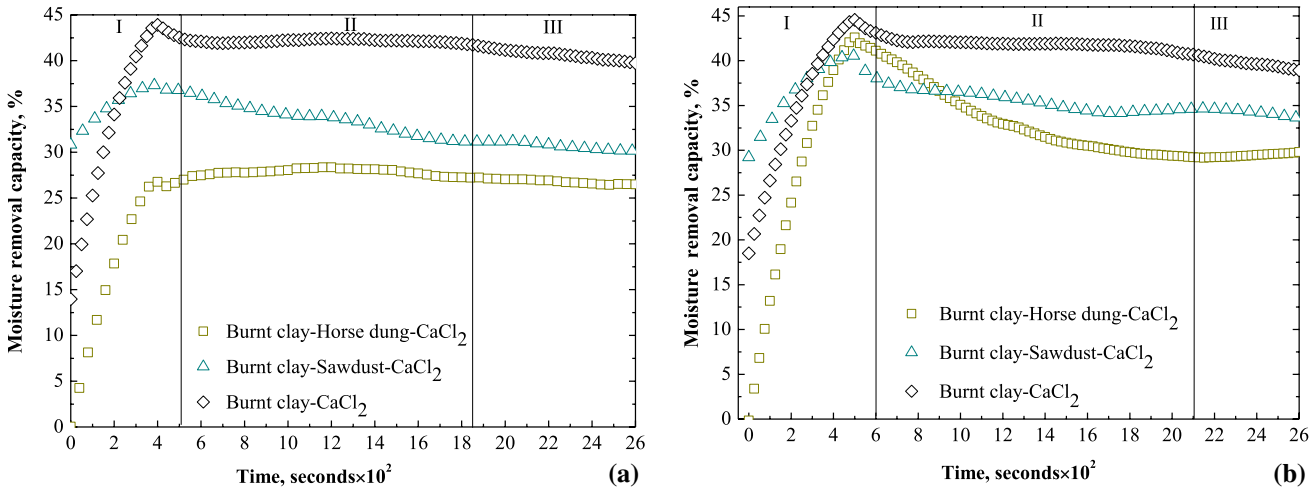

Fig. 16 Comparisons of packed and fluidized clay-additives-$CaCl_2$ beds showing slow (I), medium (II) and fast (III) dynamic regimes in adsorption

movement of the upper portion upward in a fluidized manner, while the lower bed mass moves in a quasi-static manner and resembles a packed bed state. This results in uniform adsorption during the early period of the process. The water content in the trailing layer successively increases at a rate higher than that of the upper leading layers. As the trailing layers adsorb more water vapor from the air, their mass transfer potential decreases compared to the upper layers. Therefore due to the reduced practical adsorption volume of the bed, the mass transfer coefficient decreases with time until a significant portion of the adsorption is carried out with the moving desiccants. During desorption (Figs. 18b, 19b, 20b) initially, the lower values of bed specific heat increase desorption rate, and subsequently, mass transfer coefficient increases. With progress in time, the accumulation of water vapor in the bed further increases the specific heat of the bed. The increased specific heat decreases the desorption rate and the mass transfer coefficient steadily decreases and reaches a minimum value.

7 Conclusions

In the present study, transported soil with illite clay minerals is employed to prepare low-cost composite adsorbents. The study reports the influence of pore properties, surface chemical content and specific heat on transient water vapor adsorption–desorption characteristics of desiccant bed comprising burnt clay and burnt clay-additives-$CaCl_2$ composite desiccant. The conclusions are as follows:

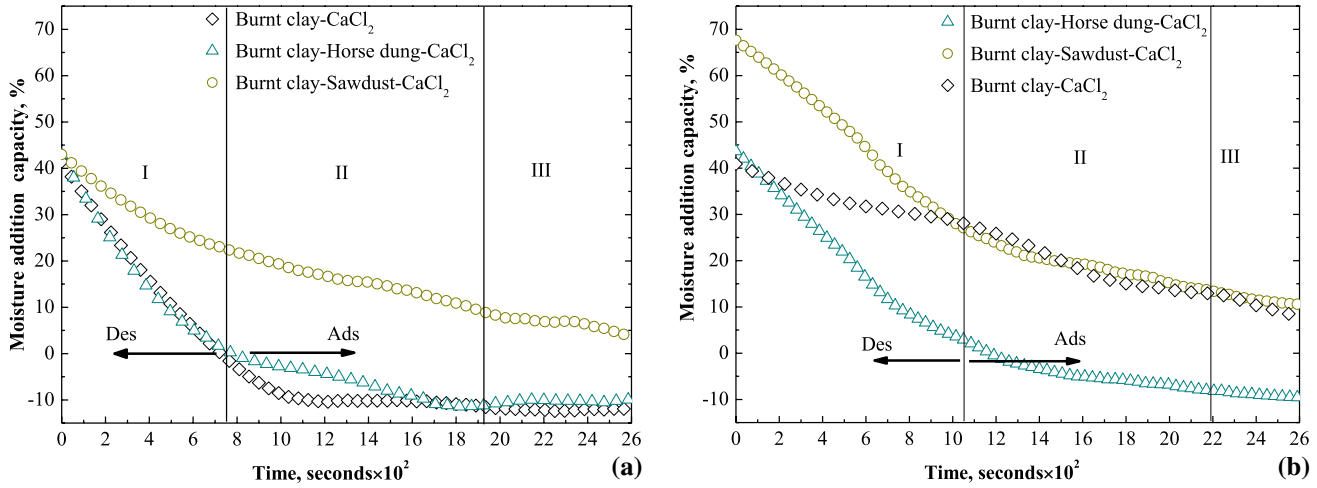

Fig. 17 Comparisons of packed and fluidized clay-additives-$CaCl_2$ beds showing slow (I), medium (II) and fast (III) dynamic regimes in desorption

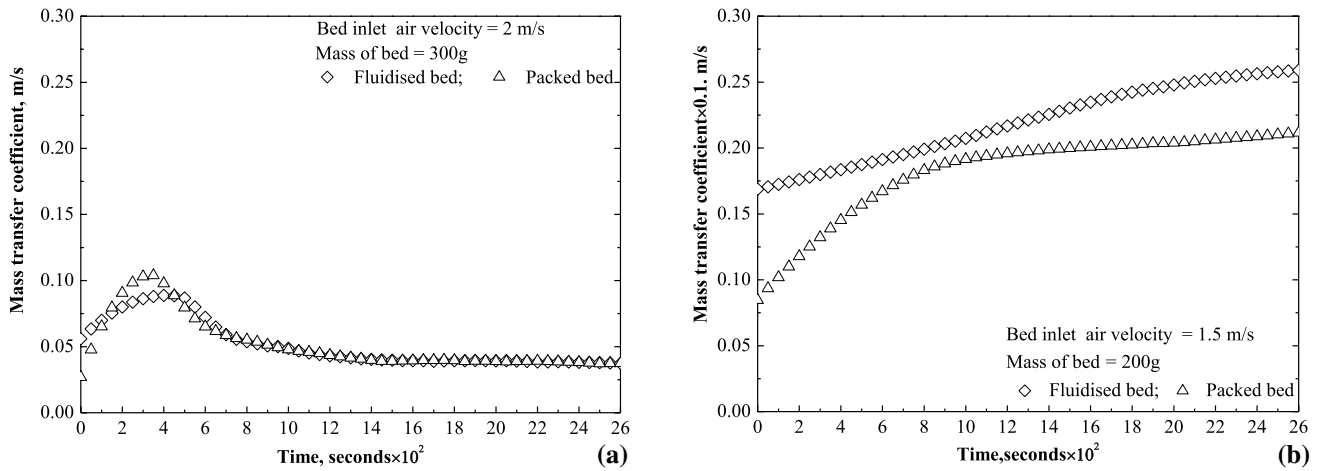

Fig. 18 Transient variation of mass transfer coefficient for burnt clay-$CaCl_2$ desiccant beds in **a** adsorption and **b** desorption

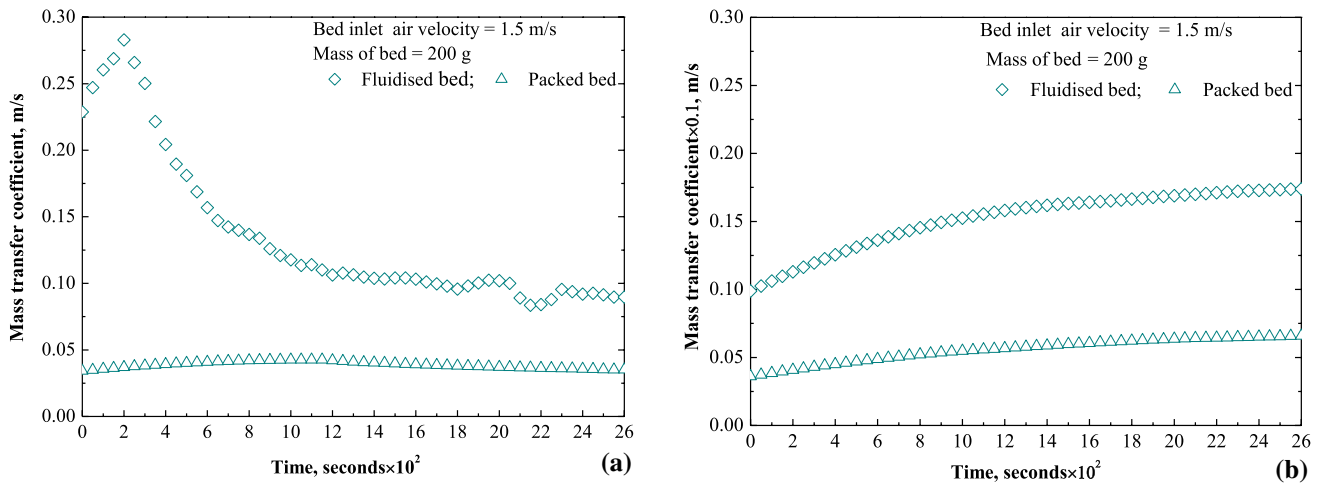

Fig. 19 Transient variation of mass transfer coefficient for burnt clay-sawdust-$CaCl_2$ desiccant beds in **a** adsorption and **b** desorption

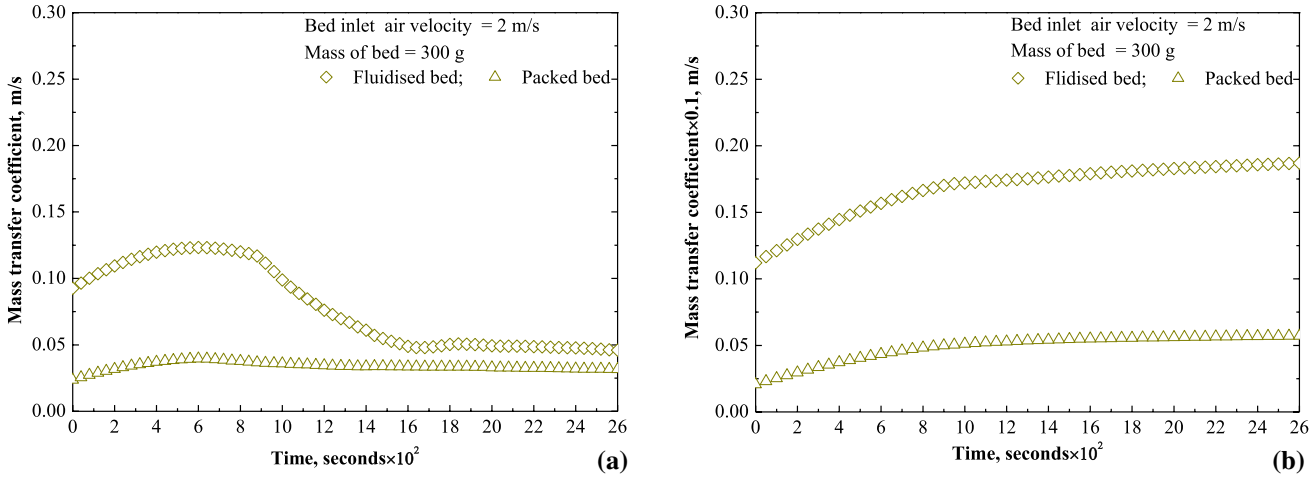

Fig. 20 Transient variation of mass transfer coefficient for burnt clay-horse dung-$CaCl_2$ desiccant beds in **a** adsorption and **b** desorption

1. Adding additives to clay increases the surface pore size and grain sizes in clay-additives composite desiccants. Higher pore volume and smaller grain sizes contribute to lower specific heat values in clay composite desiccants. In contrast, lower pore volume and larger grain sizes are attributed to higher heat capacities in clay-additives composite desiccants.
2. It has been observed that the maximum reduction in moisture content occurs in the early stages of the process for all the desiccant materials.
3. Exposure of desiccants to the low humidity of process air results in a monolayer sorption process wherein sorption takes place in primary sites of the clay-additives-based adsorbent surface.
4. The average MRC and MAC values for clay and clay-additives composite desiccants are 33.48 and 27.46%, compared to 74.92 and 76.55% for silica gel desiccant bed [29].
5. The average drop in temperature of clay and clay-additives composite desiccant bed exit air with respect to inlet air temperature is 0.80 °C (fluidized bed) and 1.80 °C (packed bed). The average increase in silica gel bed exit air temperature is 17.10 °C with respect to inlet air temperature [29]. The lower temperature of clay and clay-additives composite desiccant bed exit air than silica gel will promote the cooling energy saving in sorption-based systems.
6. Regeneration temperature as low as 55 °C demonstrates the possibility of using low-grade energy such as solar heat for clay composite desiccants reactivation.
7. The naturally available clay and materials like horse dung and sawdust, which are mostly treated as waste, can be used to prepare desiccants for humidification and dehumidification applications and have the potential to replace traditional desiccants. This leads to value addition and promotes natural materials in desiccant preparation.

Acknowledgements This research work is carried out by research facilities provided at BLDEA's V. P. Dr. P. G. Halakatti College of Engineering and Technology Vijayapur-586103, Karnataka state, India, The authors acknowledge the local pot maker of Vijayapur, for providing the transported soil, horse dung and sawdust employed here.

References

1. Zheng X, Ge TS, Wang RZ (2014) Recent progress on desiccant materials for solid desiccant cooling systems. Energy 74:280–294
2. Jain S, Dhar PL, Kaushik SC (2000) Experimental studies on the dehumidifier and regenerator of a liquid desiccant cooling system. Appl Therm Eng 20:253–267
3. Dupont M, Celestine B, Nguyen PH, Merigoux J, Brandon B (1994) Desiccant solar air conditioning in tropical climates: I—dynamic experimental and numerical studies of silica gel and activated alumina. Sol Energy 52:509–517
4. Lee SH, Lee WL (2013) Site verification and modeling of desiccant-based system as an alternative to conventional air-conditioning systems for wet markets. Energy 55:1076–1083
5. La D, Dai YJ, Li Y, Wang RZ, Ge TS (2010) Technical development of rotary desiccant dehumidification and air conditioning: a review. Renew Sustain Energy Rev 14:130–147
6. Islam MA, Pal A, Saha BB (2020) Experimental study on thermophysical and porous properties of silica gels. Int J Refriger 110:277–285
7. Uddin K, Islam MA, Mitra S, Lee JB, Thu K, Saha BB, Koyama S (2018) Specific heat capacities of carbon-based adsorbents for adsorption heat pump application. Appl Therm Eng 129:117–126
8. Wang R, Amano Y, Machida M (2013) Surface properties and water vapor adsorption–desorption Characteristics of bamboo-based activated carbon. J Anal Appl Pyrol 104:667–674
9. Qian Q, Sunohara S, Kato Y, Ahmad Zaini MA, Machida M, Tatsumoto H (2008) Water vapor adsorption onto activated carbons prepared from cattle manure compost (CMC). Appl Surf Sci 254:4868–4874

10. Saha BB, Chakraborty A, Koyama S, Aristov YI (2009) A new generation cooling device employing $CaCl_2$ in silica gel water system. Int J Heat Mass Transf 52:516–524
11. Chen CH, Schmid G, Chan CT, Chiang YC, Chen SL (2015) Application of silica gel fluidised bed for air—conditioning systems. Appl Therm Eng 89:229–238
12. Luthra K, Sadaka S (2020) Investigation of rough rice drying in fixed and fluidized bed dryers utilizing dehumidified air as a drying agent. Drying Technol 39(8):1532–2300
13. Khedari J, Rawangkul R, Chimchavee WH, J, Watanasungsuit A, (2003) Feasibility study of using agriculture waste as desiccant for air conditioning system. Renew Energy 28:1617–1628
14. Singh A, Kumar S, Dev R (2019) Studies on cocopeat, sawdust and dried cow dung as desiccant for evaporative cooling system. Renew Energy 142:295–303
15. Huashan LI, Xianbiao BU, Lingbao W, Zhenneng LU, Weibin MA (2012) Composite adsorbents of $CaCl_2$ and sawdust prepared by carbonization for ammonia adsorption refrigeration. Front Energy 6:356–360
16. Hamed AM (2003) Desorption characteristics of desiccant bed for solar dehumidification/humidification air conditioning systems. Renew Energy 28:2099–2111
17. Hamed AM (2003) Experimental investigation on the natural absorption on the surface of sandy layer impregnated with liquid desiccant. Renew Energy 28:1587–1596
18. Kumar M, Yadav A (2015) Experimental investigation of solar powered water production from atmospheric air by using composite desiccant material $CaCl_2$/saw wood. Desalination 367:216–222
19. Thoruwa TFN, Johnstone CM, Grant AD, Smith JE (2000) Novel, low cost $CaCl_2$ based desiccants for solar crop drying applications. Renew Energy 19:513–520
20. Watts KC, Bilanski K, Menzies DR (1985) Comparison of drying corn using sodium and calcium bentonite. Can Agric Eng 28:35–41
21. Biswas TD, Mukharji SK (1994) Textbook of soil science. Tata McGraw-Hill Publishing Company Limited. ISBN 0-07-462043-6
22. Fungtammasan B (2001) Prediction of minimum fluidisation velocity from correlations: an observation. Asian J Energy Environ 2:145–154
23. Hiremath CR, Katti VV, Kadoli R (2014) Experimental determination of specific heat and thermal conductivity of clay + additives + $CaCl_2$ composite desiccant. Procedia Mater Sci 5:188–197
24. Dow (2003) Calcium chloride data hand book*:* a guide to properties, forms, storage and handling. Dow Chemical Company, Michigen
25. Kline SJ (1953) The description of uncertainties in single sample experiments. Mech Eng 75:3–9
26. Holman JP (1994) Experimental methods for engineers, 6th edn. McGraw-Hill, New York
27. Robert J (1988) Moffat, describing the uncertainties in experimental results. J Exp Therm Fluid Sci 1:3–17
28. Cullity BD (1978) Elements of X-ray diffraction, 2nd edn. Addison-Wesley Publishing Company Inc., Philippines
29. Pesaran AA, Mills AF (1984) Modeling of solid-side mass transfer in desiccant particle beds. SERI/TP-252-2170. https://www.osti.gov/servlets/purl/6881795